Nodal Points, and the Eye

MICHAEL J. SIMPSON

Simpson Optics LLC, 3004 Waterway Ct, Arlington, TX 76012, USA
Corresponding author mjs1@outlook.com

Received XX Month XXXX; revised XX Month, XXXX; accepted XX Month XXXX; posted XX Month XXXX (Doc. ID XXXXX); published XX Month XXXX

The nodal points are defined using parallel object and image rays at very small angles to the optical axis, and Johann Listing described them when characterizing the eye in 1845. They are only distinct from principal points when there is a refractive index difference, but Reginald Clay used the term "nodal slide" in 1904 for equipment that uses lens rotation when measuring a lens focal length in air, and over time sketches of nodal rays at large angles have become common. These perhaps appear to support observations that input angles to the eye match image angles measured to the nodal point. Raytrace calculations confirm that this is correct to very large angles, but the relationship comes from the cornea curving around towards incoming light, angles being rescaled at the exit pupil by a constant factor, and then the retina curving around to meet the image rays. The eye has high linearity, with 1:1 angular scaling occurring at approximately the nodal point, but it is ray bundles passing through the pupil center that define the optical properties, and not paraxial nodal rays.

1. INTRODUCTION

Recent efforts to model the eye in the far periphery have led to re-evaluating optical parameters that are potentially useful for all lenses. The starting point was an evaluation into why the nodal point can be a useful reference for scaling the retinal image at very large angles, even though the nodal point of a lens system is a paraxial property [1–3]. The earlier work was for a "pseudophakic" eye where an intraocular lens (IOL) had been implanted during cataract surgery. An IOL has a single refractive index, but similar calculations are done here for a "phakic" eye that has a natural crystalline lens with a gradient index, and the results are broadly similar. One important aspect of the discussion is the fact that the eye has a highly curved retinal image surface, even though the cardinal points of a lens system are defined for plane image surfaces. A curved detector is still rarely available to lens designers, though the eye itself is frequently of interest, with recent work involving topics like virtual reality, near-eye displays, intraocular implants, contact lenses, corneal refractive surgery, and improvements in widefield imaging of the retina.

The earlier work on IOLs came about because some patients see bothersome dark shadows in their far peripheral vision. This led to finding that the far periphery had never been modeled for the eye, and that when it was modeled in raytrace software with an IOL, the main focused image is vignetted at large angles [2,4], leading to the primary image going totally dark. However, light can also miss the IOL and illuminate the retina directly, and it is likely that these characteristics are the cause of bothersome shadows with small pupils, though there is still no consensus about this as the cause of "negative dysphotopsia", as it is called clinically [2,5–8]. Matching retinal locations to visual angles in the far periphery is problematic because there is a double image effect. Raytrace evaluations showed, however, that angles measured to the second nodal point were very similar to input angles to over 70 degrees. It was not clear why that would be the case, though it seemed to be something that was generally known in ophthalmology and optometry, but not really clearly explained.

In addition to raytracing the phakic eye, the history of the nodal points and the "nodal slide" were also explored in order to try to determine how the nodal point came to be accepted as a reference point for retinal scaling, even for large angles. The nodal points themselves appear to have been originally defined for the eye, even though they are often discussed in more general terms, without using the eye as a primary example. The cardinal points are important for characterizing the "focal length" or the "power" of a thick lens optical system, and the use of the term "nodal slide" may be something that has been particularly misleading, because it is usually used in air, under conditions where a nodal point is the same as a principal point.

The discussion here is solely concerned with rotationally symmetric models for the eye, and the traditional use for the nodal point terminology. In practice, the eye has many asymmetries, though these are usually relatively modest. The eye also has astigmatism, which can be a significant aberration, and the retina does not normally have a shape that is as simple as the

sphere that is used here for an average eye. There are important recent discussions that extend the nodal point concept to asymmetric and freeform surfaces [9,10], particularly because of astigmatism, but these are not considered here.

2. HISTORICAL BACKGROUND

Johann Listing was probably the first person to properly describe nodal points in 1845, as a result of efforts to characterize the eye [11,12]. It was already known that when several lens elements are combined together then the optical properties can be described as though it is a single lens, but with the eye, the fluid on the image side made a difference. The nodal points, called *knotenpunkte* by Listing in German (plural), belong on a paraxial "cardinal point" drawing (Fig 1), though they are often misleadingly drawn on their own (Fig 2). They are points where the angle of an input ray that is projected to the optical axis to identify the first nodal point (NP1), is the same as the angle of a corresponding output ray projected back to the optical axis as though it came from the second nodal point (NP2). The ray might be called a "nodal ray" [13]. There may be more general reasons for defining a nodal ray as being any ray where the output angle is parallel to the input angle, but the discussion here is solely about the circumstances where this is tied to the nodal points, which seems to be the most common use of the term.

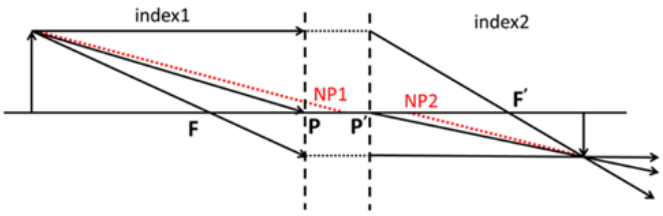

Fig. 1. Sketch of rays that define the cardinal points for very small angles (paraxial rays). The nodal points NP1 and NP2 are characterized by parallel rays, and they only differ from principal points when there is a refractive index difference. The other points are the principal points (P, P'), and the focal points (F, F'). An example of a drawing with no nodal points is fig. 258 in [14].

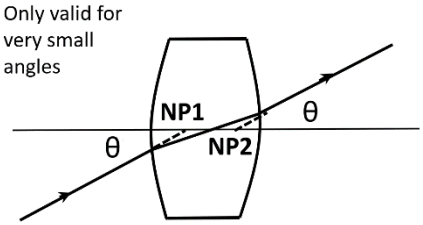

Fig. 2. Misleading sketch that is often used to illustrate the nodal points, even though for a lens in air these are really principal points. The angles are close to 30 degrees here, and there is no indication that it is only valid for very small angles. However, this does capture the fact that the discussion is only about input and output angles, and that the ray itself does not actually go through the nodal points (NP1 and NP2). An example of a drawing of this type is Fig. 2.2 in [15].

The other cardinal points are the principal points (P) and the focal points (F), where the axial separation between them is the focal length. Most lenses have air as the medium at the object and the image, and then the nodal points do not exist as independent points, but they become the same as the principal points. The terminology relating to this has probably been responsible for a lack of clarity about the nodal points. In particular, one method for measuring the focal length of a lens in air is to use a "nodal slide", and this name was given in a paper by Reginald Clay in 1904 [16], though there is also a 1903 paper by Conrad Beck that discusses methods that involve lens rotation [17] (cited by [18]). It is perhaps assumed to be obvious that if nodal points are a known concept, then the test method is also obvious, but that is not really the case. There seems to have been a half century between Listing describing the value that parallel input and output rays at an angle had for an optical system, and the establishment of test methods where a lens is rotated.

Clay's description of the test method is clear [16], and he states that he gives the important part of the equipment the name that the test is known by:

"For good work, the rotating turntable for the lens– the "nodal slide" I have called it - should be made of metal."

He does not specifically explain why he gave it this name, but he describes the principal and nodal points as being the same thing (paraphrasing very slightly to match Fig. 1)):

"If we measure … the "focal length" of the lens from F' along the axis toward the front, we shall come to another point P', which is of great importance. It is called a "principal point" or a "nodal point".

He summarizes the test method itself with this description:

"These nodal points have a very curious property. If the lens be mounted on a turntable so that it can turn about a vertical axis passing through P', and a distant object be focused on a screen at F', no motion of the lens round this axis will have any effect on the position of the image at F', which will remain perfectly stationary. Should the axis not passthrough P', but be a little in front of or behind it, the image will move to and fro as the lens is turned. It is by this property that the nodal point is found. The experiment is very striking, and can be easily repeated."

The terminology used by Clay might still be used today, and the test method seemed to rapidly become something tied to the nodal point itself, with no reference to who was involved in developing it, or how it came about. There was no mention of a test method like this in 1892 [19], and no mention at an optics conference in London in 1905, even in a paper by Beck that addressed a similar topic [20]. In that paper Beck explains in detail how the nodal point can be used to determine image properties when the eye is used with external lenses. By the time of a second London conference in 1912, Searle described more sophisticated equipment, but there was no mention of the origins of the test [21]. Searle describes it as a "nodal point" method, and although he does not specifically spell it out, the name distinguishes it from other methods for measuring the focal length in air, where three general test categories might be (a) focusing (relate object and image points, or use a known vergence), (b) magnification (compare image size to known object size), and (c) this other category, where the lens is physically rotated.

In 1905, Beck may have been attempting to deal with the language ambiguity by using the term "equivalent planes" for a lens in air, rather than using the terms principal planes and nodal planes [20,22], but this does not seem to have caught on. This is an implicit recognition that the nodal point has an importance of its own when the refractive index is different on one side. His description of the value of simplifying an optical system in air that has several lens elements is worth repeating here (even though it

does not specifically deal with nodal points) [22]) : "if, however, we take a thin single lens D or D' of a certain focal length , and place it at a position E to receive the rays of light , and then rapidly shift it to E' to discharge these rays , it will act in an exactly similar manner to the compound instrument. Such a lens can be found for all optical systems that have a focus. This lens is called the equivalent lens, and the focus of this lens is the true focus, or the equivalent focus of the compound instrument, and the two positions where the equivalent lens has to be placed, first to

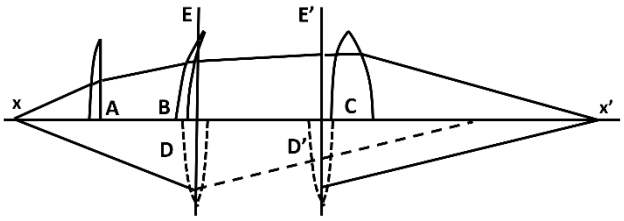

receive, and then to discharge the light, are the equivalent planes of this compound instrument".

Fig. 3. Beck's illustration of how a compound lens system in air with 3 lenses (top (A, B, and C)) can be represented optically by a single thin lens that moves rapidly from D to D' (bottom).

Any consideration of the nodal point of the eye has these concepts in the background, and two additional aspects are also worth mentioning. One is simply that there do not normally seem to be sketches that depict the rotation of a lens. Fig. 1 is just for a single point on an object, and Figure 4 attempts to illustrate how the object and the image do not move when the lens is rotated about NP2. If the top of the object is considered, then when the lens is rotated, different nodal rays connect the two points. This is not necessarily intuitively obvious, because usually when we rotate a lens we would also be rotating a camera, yet here the axis on the image side does not move, and a new NP1 is defined for the new nodal ray with a tilted lens. The figure also illustrates some of the approximations involved in the whole discussion. The cardinal point concepts are for very small angles, yet when the nodal slide test is done, the image that is viewed is often relatively large, while at the same time the angle of rotation is very small. There is a distinction between the angle of the field of view, and the angle of rotation of the optical axis. There is also an inherent lack of clarity about things like whether the image is in focus as the lens rotates, though the assumption is that the rotation angles are small.

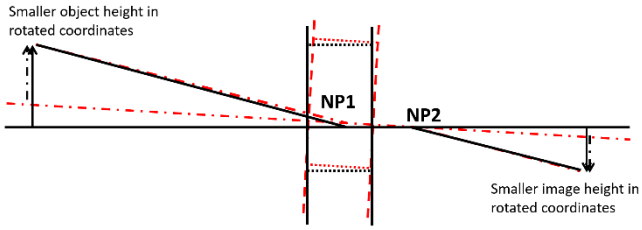

Fig. 4. In a test with a nodal slide, the lens rotates, but the object and image do not move when the rotation is about NP2. Depicting just the nodal rays for the rotated lens (dashed) reveals limitations of the normal cardinal point sketch, where object and image planes tilt. The ray direction from NP2 to the image is the same for both orientations, but the object height and NP1 location change.

Also, even though the simplicity of the cardinal point description is correct for something like a complex photographic lens used in air, the practical details can affect this type of evaluation. The focal length is typically defined for collimated light, and with complex lenses it can change for different object distances. The internal limiting aperture of the lens can also have an effect on the image as the field angle changes, and the effect of this may also vary for different object distances. The concept of the nodal point has been mentioned specifically with respect to panoramic photography, where there is interest in stitching together multiple images after a camera is rotated [23]. This is analogous to the discussion about the eye later, with the ray pencil that passes through the center of the aperture being the most important thing that determines the location of the image for that field angle and focus. The characteristics of the overall optical design may not match the paraxial situation for collimated light.

A second imaging aspect that is different for the eye is the immersion of the internal lens in fluid (with the aqueous and vitreous media having very similar refractive index values). The power of a lens in air is often simply 1/(focal length), or 1/f,' , but the actual definition is n'/f', where n' is the refractive index of the image medium. The value of 1/f' for the whole eye is about 45 D, but the power of the whole eye is about 60 D, and this is the effect that is captured by the nodal point, with the reference point moving closer to the image, by a distance that is proportional to the refractive index value.

If somebody new to the topic was trying to understand the "nodal points" of the eye, they might come across the sketch in Figure 2. Even the fact that the nodal points are described for a lens in air introduces some confusion, since the nodal points have to be different from the principal points for the eye. The cardinal point drawing in Fig. 1 has redundancy anyway for a lens in air, because only 2 of the 3 rays are needed to find the off-axis image. For a lens in air, the "nodal" terminology is implicitly identifying the parallel rays traveling at an angle to the axis. This is useful, but it also detracts from a different use of the word, for a similar purpose, when there are different refractive index values.

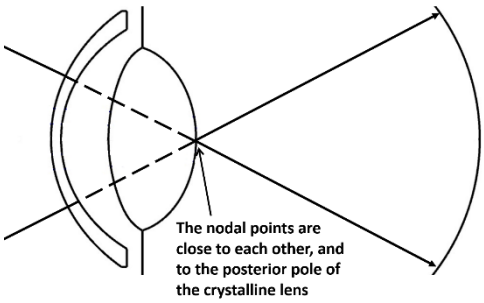

Fig. 5. A sketch that is sometimes used to illustrate the equivalence of input angles and angles to NP2 at the retina., where the nodal points are very close together, and also very close to the lens posterior pole. This turns out to be a useful approximation to very large angles to relate input angle to retinal image points, but not because of paraxial nodal point considerations. An example of a similar conceptual sketch is Fig. 2.15 in [24].

A valuable use for angular scaling is illustrated for the eye in Fig. 5, which approximately relates the input angle to the corresponding retinal region. The rationale for this illustration is usually based on paraxial imaging and the nodal points, but the

calculations here show that the concept is generally also correct for very large input angles, using chief rays that pass through the center of the pupil, rather than actual nodal rays. The drawing appears to depict rays that relate object and image points for a range of angles, but they are really just 2 lines that depict the input and output angles. The sketch uses useful approximations for small angles, where the two nodal points are very close together, and also approximately located at the posterior surface of the natural crystalline lens, so the points are all superimposed.

An alternative concept that is related to a "paraxial" approximation is not explored here in detail, but it has some relevance to the phakic eye. The usual description for the paraxial approximation is that the rays must be at small angles to the optical axis [25, p238]. However, the characteristic that is the most important is that the angles of incidence to the surfaces should be small, so that $\tan(\theta) \sim \sin(\theta) \sim \theta$, if θ is the angle of incidence. For the phakic eye, the angles of incidence tend to be relatively close to normal incidence, even for very large input angles, because of the curvatures of the cornea and the crystalline lens. This is indirectly evaluated in the results section, where there are data that explore the angular range over which nodal rays go through the paraxial nodal points.

3. METHOD

Zemax OpticStudio optical design software (Zemax.com) was used to evaluate a schematic model of an average 70 year old phakic eye that had been used before [4]. The crystalline lens for the older eye was modeled using a user-defined surface from the study by Akram et al. [26], based on the work by Bahrami and Goncharov [27], and it was further modified to have an aspheric anterior surface that attempted to match the crystalline lens at large diameters. This age was used because it is a typical age for cataract surgery, where the recent questions about "negative dysphotopsia" and "far peripheral vison" have not yet been fully resolved. A widely used gradient index eye model for an average eye that was described by Liou and Brennan was also evaluated [28], which represents an age of 45. The crystalline lens grows throughout life, with the lens pushing the iris forward as it grows, and with compensating changes in the gradient refractive index that minimize changes in refractive error. The aqueous and lens thickness were 2.57 mm and 4.7 mm for the older eye, and 3.16 and 4 mm for the younger one (though the younger eye also has an unusually thin cornea of 0.5 mm).

Only chief rays that pass through the center of the aperture stop were evaluated, with the Zemax "ray aiming" routine used to set the direction. Rays were traced for a range of angles using a Zemax macro, which also determined ray intersections with the retina and calculated angles from there to 3 axial locations: the exit pupil, the second nodal point (NP2), and the center of the 12 mm diameter retinal sphere. The angles were evaluated relative to the optical axis, and 5 degrees would have to be added to the input ray angles to give angles relative approximately to the visual axis (angle alpha).

As a separate calculation, rays that met the nodal ray criterion were found, where the output ray was parallel to the input ray. The paraxial discussion implicitly assumes that nodal rays go through the nodal points, but it had been found that this was not the case for the pseudophakic eye when the input angle was larger than a few degrees [1]. The ray intersections with the cornea and iris were determined here, in addition to the axial intersections, with no constraint on the off-axis radius at either the cornea or the iris.

4. RESULTS

The 70 year old phakic eye was found to have broadly similar properties to the pseudophakic eye that had been evaluated earlier [4]. Fig 6 shows chief rays at several input angles that pass through the center of the pupil, and they are rescaled by a fairly constant factor of about 0.8 at the exit pupil over 70 degrees. Three axial reference points are of interest, with the exit pupil at 3.2 mm, NP2 at 7.4 mm and the center of the retinal sphere at 11.5 mm from the anterior corneal surface. The angles from the image points on the retina to these axial locations are plotted in Fig. 7.

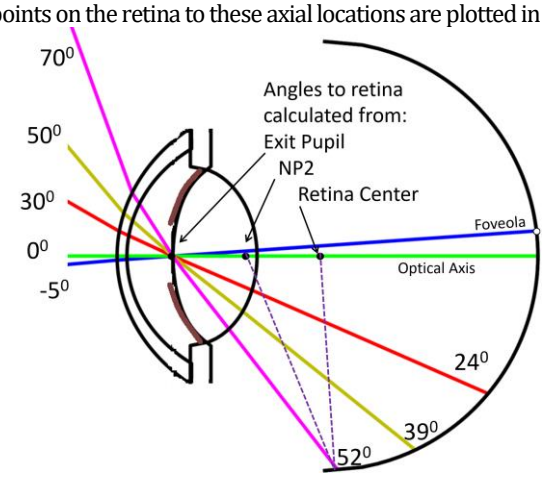

Fig. 6. Drawing of right eye from above, labeled with chief ray angles relative to the optical axis. Three axial points of interest are marked, and the dotted lines indicate how the additional angles are calculated.

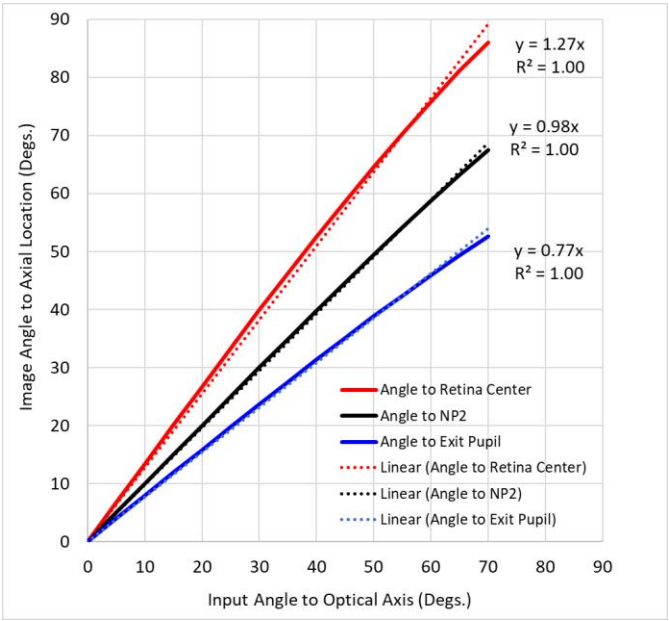

Fig. 7. Output angles from the chief ray retinal intersection to the 3 axial points of interest plotted against input angles to the eye, along with linear curve fits forced to go through 0.

The lines in Fig. 6 are actual chief rays, and they represent the directions that ray bundles travel in order to create the retinal image. The lines drawn to the two other axial points are not rays

at all, and they merely indicate the angles to those points. All three relationships are very linear, but with different slope values in Figure 7. When the second nodal point NP2 is used as the reference, the slope is approximately 1:1, even though none of the rays are nodal rays. It can also be seen in Fig. 6 that the input rays projected to the optical axis at larger angles do not all meet in a point, which would be a requirement if the nodal point criterion was relevant at all. Even a ray at a very low angle of 5 degrees would not match the nodal point criterion that is envisaged by the cardinal point sketch of Fig. 1, because the rays are directed here to the center of the aperture, and not towards the first nodal point.

The results for the other eye model (age 45) were similar to the ones that are plotted, with the exit pupil at 3.7 mm, NP2 at 7.4 mm and the center of the retinal sphere at 12 mm from the anterior corneal surface. The slopes of the 3 lines corresponding to Fig. 7 were 0.80, 0.99, and 1.32. Evaluating the linearity further, Figure 8 plots the ratio of the retinal angles to the input angles for the 3 axial locations, for both the phakic eyes. This describes the angular linearity in a different manner, and it can be seen that there is more of a change when the center of the sphere is used as the reference (though angles are also larger there). The scale factor shows least change between the two eyes when the nodal point is used as the reference.

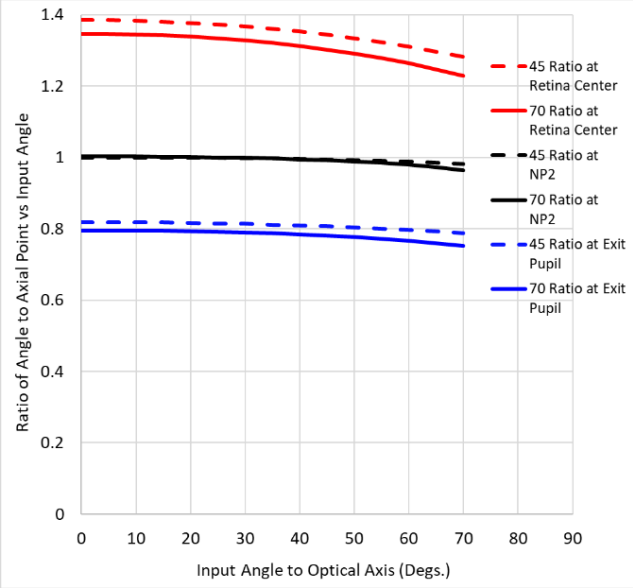

Fig. 8. Ratio of output angle to input angle for the 3 axial locations for both the 70 year-old and 45 year-old eyes (labeled 70 and 45).

Fig. 9 plots some additional parameters that are related to the overall discussion about nodal points, where raytracing has been used to find rays where the input and output angles are parallel. This is the nodal ray criterion, and the axial points that correspond to the definition of the traditional nodal points were determined (called point 1 and point 2). The curves in black are for the 70 year old eye that is the main model here, and the curves in red are for a similar eye with an intraocular lens instead of a crystalline lens that had been evaluated previously [1]. In Fig. 9(a), the radial distance from the optical axis rapidly tracks off to the side as the input angle increases. This corresponds to a diameter at the cornea of about 10 mm by about 50 degrees, which is already approaching the diameter of the clear cornea (about 12 mm). The corresponding diameters at the iris are close to 6 mm, which is a typical diameter for an IOL.

Fig. 9(b) plots the axial locations of the ray intersections, called point1 and point2. For small angles these are the same as the nodal points, but as the angle increases, for the pseudophakic eye with an IOL the points no longer correspond to the nodal points. With the phakic eye, however, the curves are much flatter, and up to about 50 degrees the traditional nodal points are reasonable approximations. This is consistent with the concept mentioned earlier, that if the angle to the lens surfaces is close to normal incidence, which it is with a crystalline lens, then the rays also have "paraxial" properties at some level. The rays cannot deviate very much, because they are not being refracted very much at the surfaces. At about 50 degrees, however, a position is reached where there are no longer any rays that meet the criterion. The calculations were done with no pupils, and larger input angles were tried, but there were no parallel output angles. The rays at very large angles are also the most aberrated rays, and not the ones that correspond to the main focused image location, which is captured instead by the chief ray that is used for the main calculations.

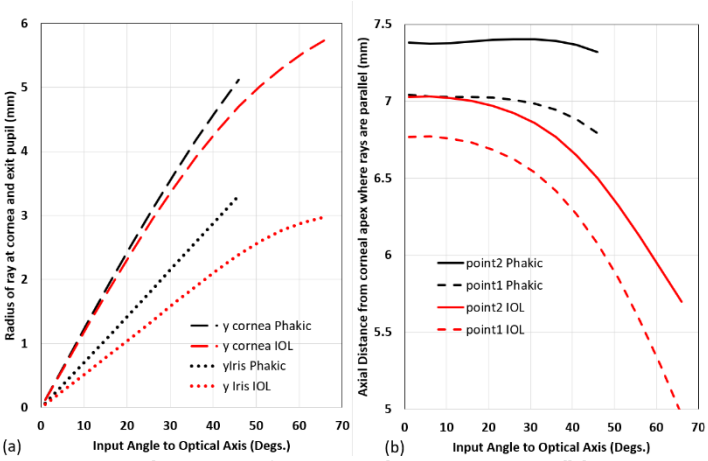

Fig. 9. Ray characteristics for situation where input ray is parallel to image ray, for phakic eye model, and eye model with intraocular lens instead. (a) Radial distances from optical axis at cornea and exit pupil. (b) Axial intersection distances from corneal apex. Point1 and Point2 are the nodal points for small angles.

A comparison between phakic and pseudophakic eyes warrants more evaluation than has been done here. There is an approximately 1:1 correspondence between input angles and their own second nodal points for chief rays over a 70 degree range of input angles. However, the phakic eye has an iris that is more anterior at 3.1 mm from the anterior corneal vertex, and in contact with a gradient index crystalline lens with very rounded surfaces that is 4.7 mm thick. The pseudophakic eye has a deeper iris at 4 mm, a gap between the iris and the IOL of 0.5 mm, and a high index lens with much flatter surfaces that is only 0.7 mm thick. The raytrace results show that these two types of eye have broadly similar properties for large angles, but there does not appear to be a body of work where these types of details have been evaluated.

5. DISCUSSION

The calculations here for the older phakic eye are broadly similar to those for a pseudophakic eye, and they perhaps confirm what was thought to be already known, that the second nodal point is a useful reference for identifying the location on the retina that corresponds to a particular input angle. A ruler can be used on a cross-sectional drawing of an eye. Simply rotating it to the right angle, and moving it to go through the posterior pole of the crystalline lens (or an estimated small distance in front of it), a line can be drawn that indicates approximately where light at that visual angle is incident on the retina [29]. This is a very useful simplification for an average eye. A range of eyes is not considered here, and the retina will usually be elliptical, and perhaps also asymmetric, but this could always be used as a first approximation.

This scaling seems to have little to do with the definition for the nodal point. The overall optical design of the eye for large angles is that the cornea curves around toward light entering at an angle, which helps to provide angular linearity for ray bundles that pass through the pupil and head towards the image. And then the retina curves around to meet the image, which acts to maintain the linearity with respect to angle.

The scaling at large angles depends on a geometrical construction that has a special property of transferring angles from one location on the optical axis to another. Figure 10 depicts the geometry that relates angles at either the pupil center or the nodal point to the angle at the center of a spherical retina. The simple equation gives the approximate relationship, but this does not appear to be easily derived using standard trigonometry, and it is not known if this relationship has previously been described. For angles θ_1 at dz1 and θ_2 at dz2 the relationship is $\theta_2 = \theta_1 * (R + dz1)/(R + dz2)$. A suggestion that the geometry might be related to "inscribed angles" led to evaluating the error when the distance is varied from the center to the edge for a fixed retinal point, and even for an angle of 90 degrees the maximum error is only about 4 degrees (and only about half that for the locations of interest).

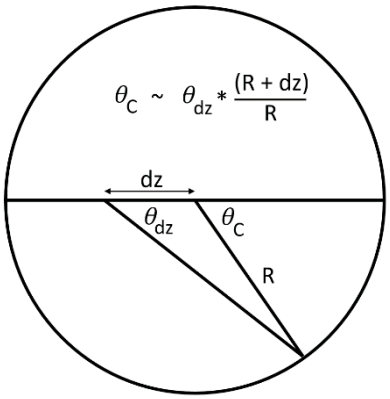

Fig. 10. The simple geometry that rescales the angles to different axial locations.

The simplified analysis here addresses only one aspect of the imaging properties, which is really the distortion characteristic. The effects of things like defocus and aberrations are not specifically addressed. A related aspect is the shape of the entrance pupil, which changes significantly at large angles. This was evaluated in detail by Fedtke et al. [30], and the same automatic Zemax routine has been used here to find the pupil center. This is an excellent feature of Zemax, but otherwise Zemax does not really envisage that images might be formed on curved image surfaces, and it provides very limited capabilities. Currently most image surfaces are plane, apart from the eye, but perhaps this will change in the future, which would provide an additional degree of freedom for lens design.

The stimulus for this evaluation was visual phenomena at very large angles reported by pseudophakic patients, which is a topic of active research [8,31,32]. Unfortunately, the linearity with angle discussed here does not extend perfectly to the very far peripheral region that is thought to be important for negative dysphotopsia, but similar angular properties were found for these lower angles by Drasdo et al [33] in a paper concerned specifically with the modest nonlinearity at extremely large visual angles, which was also evaluated in more detail by Suheimat et al [34]. Image linearity with angle over a very large range seems to be often assumed for the eye, with linearity being important for psychology aspects of vision [35]. However, the optical characteristics of the eye that make this possible are not necessarily evaluated anywhere together. The Drasdo et al and Suheimat et al papers compare distances along the retina from the foveola to input angles. These distances are directly proportional to the measurement of angles to the center of the retinal sphere that are calculated here, because they are arcs. The rescaling of angles at the exit pupil are visible in diagrams in these papers, but not remarked on, and although the nodal point is mentioned by Drasdo et al, it is not clear what was calculated.

A related topic is the field of fundus photography, which has recently expanded to include very widefield retinal imaging. This is somewhat independent of vision research, with practitioners perhaps more often looking for visual characteristics of the retina itself, rather than actually matching up visual measurements to retinal locations. Scaling might be only approximate, and there is a distinct lack of clarity about the scaling of modern widefield imaging systems [36]. The patent literature also has some examples of lenses used to image the retina, and linearity with respect to angle seems to be recognized, but not specifically discussed [37]. Recent papers relating to widefield fundus imaging provide useful examples for this type of imaging system, because they use standard "indirect ophthalmoscopy" lenses to relay the curved retinal surface out to a flat surface in front of the eye, where it is then relayed to a camera [38,39]. Lenses like this are used routinely in an ophthalmic clinic anyway, where the image will be viewed directly by the clinician, and it is likely that strict linearity is not required. The eye will normally also have significant peripheral astigmatism. When actual models of the eye are used for calculations, the nodal points are not used, such as in a recent study by Atchison et al of eccentric autorefractors, which includes angles up to 40 degrees [40].

The history and terminology relating to the nodal point have been explored because these seem to have an effect on discussions

about scaling. The nodal point is particularly relevant for the eye because the image is in fluid, yet it is only applicable for very small angles. At the same time, the term is used widely for lens measurements in air, where the only relevance really is that an angle is involved. And lenses are also often sketched in air to illustrate the nodal ray criterion, with large angles being used to make them clear. This perhaps creates an impression that they are valid for larger angles than they are. The actual situation is somewhat different, with image scaling being primarily determined by light passing through the pupil center.

The discussion here does not directly further the original purpose of this work, which was to scale the far peripheral retina in the pseudophakic eye, but it solidifies the eye characteristics that scale the retina as far as the equator. This is a useful reference point anyway, with light entering the eye at about 70 degrees being imaged there. A recent paper related to cartography may unexpectedly have some relevance to this topic, with a description of how a flat map of the earth could be created [41] . No mention of the eye is made, but the concept is that the surface of the earth can be scaled using azimuthal angles relative to the center, and the angles are then represented by locations on a flat polar plot. The eye is a somewhat similar globe, and a wide-angle retinal image that was scaled using the center of the retinal sphere could be displayed in the same manner. A similar concept is also used for the standard charts that are used to record visual fields. When you get to the equator of the flat map though, the map is turned over, and it continues on the other side. The authors describe how this gives realistic distances for separations between points, and it highlights the fact that initially the further you get from the poles on a sphere, the further apart points on lines of latitude become. After the equator though, the points start getting closer together again. Standard visual fields only go to 90 degrees, so this effect may not have been noted (though the limit on the temporal side of the visual field is nominally taken to be 115 degrees [3], and this is a region of vision that is never measured). With a wide-field fundus image, if it goes past the equator, it is not clear how this is addressed.

The main finding behind this discussion might be that the linearity with angle that appears to be widely assumed for the eye has perhaps not been fully explored, particularly for very large angles. Discussions that refer to the nodal point as a reference point for angles at the retina seem to be correct, even though the rationale for this seems to come from paraxial sketches, where the angles are very small, the retina is flat, and there is no limiting aperture. The eye is primarily a small globe instead, and the spherical shape is very important for the linear scaling.

Funding. This paper is funded by Simpson Optics LLC with no external funding

Acknowledgments. Grateful thanks to Professor Gott for the suggestion about the included angle, and to an anonymous reviewer for comments about the broader aspects relating to paraxial optics.

Disclosures. MJS: Simpson Optics LLC (E).

Data availability. Data underlying the results presented in this paper are not publicly available at this time but may be obtained from the author upon reasonable request.

References

1. M. J. Simpson, "Scaling the retinal image of the wide-angle eye using the nodal point," Photonics **8**, 1–9 (2021).
2. J. T. Holladay and M. J. Simpson, "Negative dysphotopsia: Causes and rationale for prevention and treatment," J. Cataract Refract. Surg. **43**, 263–275 (2017).
3. M. J. Simpson, "Mini-review: Far peripheral vision," Vision Res. **140**, 96–104 (2017).
4. M. J. Simpson, "Intraocular lens far peripheral vision: Image detail and negative dysphotopsia," J. Cataract Refract. Surg. **46**, 451–458 (2020).
5. L. Werner, "Dysphotopsia , a lingering issue after cataract surgery : effect of IOL optic size," J Cataract Refract Surg **48**, 1–2 (2022).
6. S. Masket and N. R. Fram, "Pseudophakic Dysphotopsia: Review of Incidence, Cause, and Treatment of Positive and Negative Dysphotopsia," Ophthalmology **128**, e195–e205 (2021).
7. J. C. Erie, M. J. Simpson, and M. H. Bandhauer, "Effect of a sulcus-fixated piggyback intraocular lens on negative dysphotopsia: Ray-tracing analysis," J. Cataract Refract. Surg. **45**, 443–450 (2019).
8. J. C. Erie, M. J. Simpson, and M. A. Mahr, "Effect of a 7.0 mm intraocular lens optic on peripheral retinal illumination with implications for negative dysphotopsia," J. Cataract Refract. Surg. **48**, 95–99 (2022).
9. W. F. Harris, "Cardinal points and generalizations," Ophthalmic Physiol. Opt. **30**, 391–401 (2010).
10. W. F. Harris, "Nodes and nodal points and lines in eyes and other optical systems," Ophthalmic Physiol. Opt. **30**, 24–42 (2010).
11. J. B. Listing, *Beitrag Zur Physiologischen Optik* (1845).
12. H. von Helmholtz, *Helmholtz's Treatise on Physiological Optics, v1 (3rd Ed. from 1909 Translated to English 1924), Ed. J Southall*, 3rd ed. (Optical Society of America, 1924).
13. D. A. Atchison and G. Smith, *Optics of the Human Eye* (Butterworth-Heinemann, 2002).
14. W. H. . Fincham and M. H. Freeman, *Optics*, 8th ed. (Butterworth, 1974).
15. W. J. Smith, *Modern Optical Engineering*, 2nd ed. (McGraw-Hill, 1990).
16. R. S. Clay, "The Practical Testing of Photographic Lenses," The Photo-Beacon **XVI**, 109–119 (1904).
17. K. Beck, "Eine neue methode der objectivprufung," Jahrb. für Photogr. und Reproduktionstechnik **17**, 257–274 (1903).
18. S. Czapski, *Grundzuge Der Theorie Der Optischen Instruments Nach Abbe* (Verlag von Johann Ambrosius Barth, 1904).
19. S. P. Thompson, "The Measurement of Lenses," J Soc. Arts **XL**, 22–39 (1892).
20. C. Beck, "The Consideration of the Equivalent Planes of Optical Instruments," in *The Proceedings of the Optical Convention* (Norgate & Williams, Covent Garden, London, 1905), pp. 9–18.
21. G. F. C. Searle, "DEMONSTRATION OF LABORATORY APPARATUS AND EXPERIMENTS," in *The Proceedings of the Optical Convention* (University of London Press, 1912), pp. 161–172.
22. C. Beck, "The Theory of the Microscope," J Soc Arts **LVI**, 105–120, 129–141, 161–176, 181-194 (1907/1908) (1908).
23. R. Littlefield, "Theory of the "No-Parallax" Point in Panorama Photography," https://www.janrik.net/PanoPostings/NoParallaxPoint/TheoryOfTheNoParallaxPoint.pdf.
24. A. G. Bennett and R. B. Rabbetts, *Clinical Visual Optics*, 1st ed. (Butterworths, 1984).
25. D. A. Atchison and G. Smith, *Optics of the Human Eye* (Elsevier

Science, 2002).
26. M. N. A. Akram, R. C. Baraas, and K. Baskaran, "A wide-field emmetropic human eye model based on ocular wavefront measurements and geometry-independent gradient index lens," J Opt Soc Am A **35**, 1954–1967 (2018).
27. M. Bahrami and A. V Goncharov, "Geometry-invariant GRIN lens: finite ray tracing," Opt. Express **22**, 27797–27810 (2014).
28. H. L. Liou and N. a Brennan, "Anatomically accurate, finite model eye for optical modeling.," J. Opt. Soc. Am. A. Opt. Image Sci. Vis. **14**, 1684–95 (1997).
29. M. J. Simpson, "Nodal Points and the Eye," in *ARVO Annual Meeting, Denver, CO* (2022).
30. C. Fedtke, F. Manns, and A. Ho, "The entrance pupil of the human eye: a three-dimensional model as a function of viewing angle.," Opt. Express **18**, 22364–22376 (2010).
31. L. van Vught, G. P. M. Luyten, and J.-W. M. Beenakker, "Distinct differences in anterior chamber configuration and peripheral aberrations in negative dysphotopsia," J. Cataract Refract. Surg. **46**, 1007–1015 (2020).
32. M. J. Simpson, "Simulated images of intraocular lens negative dysphotopsia and visual phenomena," J. Opt. Soc. Am. A **36**, B44–B51 (2019).
33. N. Drasdo and C. W. Fowler, "Non-linear projection of the retinal image in a wide-angle schematic eye.," Br. J. Ophthalmol. **58**, 709–14 (1974).
34. M. Suheimat, H. Zhu, A. Lambert, and D. A. Atchison, "Relationship between retinal distance and object field angles for finite schematic eyes," 1–7 (2016).
35. H. Strasburger, "On the cortical mapping function – visual space, cortical space, and crowding," bioRxiv **//doi.org/**, doi: https://doi.org/10.1101/621458; (2019).
36. X. Yao, D. Toslak, T. Son, and J. Ma, "Understanding the relationship between visual-angle and eye-angle for reliable determination of the field-of-view in ultra-wide field fundus photography," Biomed. Opt. Express **12**, 6651 (2021).
37. D. A. Volk, "INDIRECT OPHTHALMOSCOPY CONTACT LENS DEVICE WITH COMPOUND CONTACT LENS ELEMENT," U.S. patent 5,523,810 (1996).
38. D. Toslak, T. Son, M. K. Erol, H. Kim, T.-H. Kim, R. V. P. Chan, and X. Yao, "Portable ultra-widefield fundus camera for multispectral imaging of the retina and choroid," Biomed. Opt. Express **11**, 6281 (2020).
39. S. Ni, T.-T. P. Nguyen, R. Ng, S. Khan, S. Ostmo, Y. Jia, M. F. Chiang, D. Huang, J. P. Campbell, and Y. Jian, "105 degree field of view non-contact handheld swept-source optical coherence tomography," Opt Lett **46**, 5878–5881 (2021).
40. D. A. Atchison, M. Suheimat, S. Zacharovas, and C. E. Campbell, "The use of autorefractors using the image-size principle in determining on-axis and off-axis refraction. Part 2: Theoretical study of peripheral refraction with the Grand Seiko AutoRef/Keratometer WAM-5500.," Ophthalmic Physiol Opt 00:1–8. (2021).
41. J. R. Gott, D. M. Goldberg, and R. J. Vanderbei, "Flat Maps that improve on the Winkel Tripel," ArXiv https://arxiv.org/ftp/arxiv/papers/2102/2102.08176 (2021).